

Evolution history of the Neoproterozoic eclogite-bearing complex of the Muya dome (Central Asian Orogenic Belt): Constraints from zircon U–Pb age, Hf and whole-rock Nd isotopes



V.S. Shatsky ^{a,b,c,*}, V.G. Malkovets ^{b,d}, E.A. Belousova ^e, S.Yu. Skuzovatov ^a

^a Vinogradov Institute of Geochemistry SB RAS, Favorskogo str. 1A, Irkutsk 664033, Russia

^b Institute of Geology and Mineralogy SB RAS, Koptyug ave. 3, Novosibirsk 630090, Russia

^c Novosibirsk State University, Pirogova st. 2, Novosibirsk 630090, Russia

^d The Pheasant Memorial Laboratory for Geochemistry and Cosmochemistry, Institute for Study of the Earth's Interior, Okayama University, Misasa, Tottori 682-0193, Japan

^e Australian Research Council Centre of Excellence for Core to Crust Fluid Systems/GEMOC, Macquarie University, Herring Road, North Ryde, Sydney, NSW 2109, Australia

ARTICLE INFO

Article history:

Received 21 August 2014

Received in revised form
30 December 2014

Accepted 29 January 2015

Available online 9 February 2015

Keywords:

Central Asian Orogenic Belt
Continental subduction
Zircon
U–Pb dating
Hf isotopes

ABSTRACT

U–Pb dating and Hf-isotope analysis of zircons and whole-rock Nd-isotope analyses were carried out on country rocks of the eclogite–gneiss complex of the North Muya dome in the Anamakit–Muya zone of the Baikal Muya accretionary fold belt. Zircons from garnet–biotite gneisses (Qtz + Kfsp + Pl + Bt + Grt) and garnet–biotite–muscovite schist (Pl + Kfsp + Bt + Mu + Grt + Qtz) were dated using the LA-ICP-MS technique. Based on U–Pb isotope data and CL images zircon grains were divided into three groups: detrital, magmatic and metamorphic zircons. Metamorphic zircons display no zoning or the cloudy zoning. The grains morphology together with the well-developed oscillatory zoning clearly identifies the igneous origin of magmatic zircons. The metamorphic zircons (ages 576–680 Ma) have Th/U ratios varying from 0.271 to 0.004, whereas the ratio in magmatic zircons ranges from 0.779 to 0.11. Magmatic zircons from granite–gneisses of the North Muya dome exhibit a relatively narrow spread in the crystallization age with the major peak at ca 764 Ma. Younger ages are interpreted as due to the partial resetting of U–Pb system during the subsequent metamorphic evolution. Detrital zircons from two-mica schist sample Mu-93-10 give ages of 1.88–2.66 Ga. The oldest detrital zircon from this sample plots near concordia and has a $^{207}\text{Pb}/^{206}\text{Pb}$ age of 3.2 Ga. Zircons from this sample are characterized by the widest scatter of $\varepsilon_{\text{Hf}}(t)$ values (from +13.9 to –15.3) and T_{DM}^{C} model ages (0.82–3.86 Ga). Zircons from other samples have a much narrower ranges of $\varepsilon_{\text{Hf}}(t)$ (+11.6 to –0.7) and T_{DM}^{C} (0.85–1.52 Ga). The involvement of older crustal material is also evident from the whole-rock Nd isotopic compositions. The gneisses and schists exhibit a range of Nd isotopic compositions with $\varepsilon_{\text{Nd}}(t)$ values ranging from –3.5 to +3.6 and $t_{\text{Nd(DM)}}$ from 1.64 to 1.09 Ga. The integration of the Hf-isotope data with the age spectra provides with the first evidence for the existence of Mesoarchean crust in the Baykal–Muya sector of the Central Asian Orogenic Belt.

© 2015 Elsevier B.V. All rights reserved.

1. Introduction

Continental subduction plays an important role in the evolution of accretionary orogens ([Cawood et al., 2009](#)) at the final stage of an ocean's closure and collision. In this context, studies of eclogite-bearing metamorphic complexes of orogenic belts,

which mark these final stages of subduction and collision of continental crust, is of great interest ([Ernst, 2001](#); [Liou et al., 2009](#)). In the Central Asian Orogenic Belt, which is one of the largest accretionary terranes on the Earth ([Windley et al., 2007](#)), eclogite-bearing complexes occur in the Hercynian (Middle-Late Paleozoic), Caledonian (Early Paleozoic) and Baikalian (Neoproterozoic) orogens ([Dobretsov et al., 1989](#)). The oldest eclogites are found in the North Muya dome ([Shatsky et al., 2012](#)), located in the Anamakit–Muya zone of the Baikal Muya accretionary fold belt (BMB) within the Baikalian orogen ([Rytsk et al., 2011, 2007](#)) ([Fig. 1](#)). Reconstruction of the geodynamic evolution of the Baikal Muya Belt is still a subject of intense debate ([Rytsk et al., 2011](#)).

* Corresponding author at: Vinogradov Institute of Geochemistry SB RAS, Favorskogo str. 1A, Irkutsk 664033, Russia. Tel.: +7 3952 426600; fax: +7 3952 427050.

E-mail address: shatsky@igc.irk.ru (V.S. Shatsky).

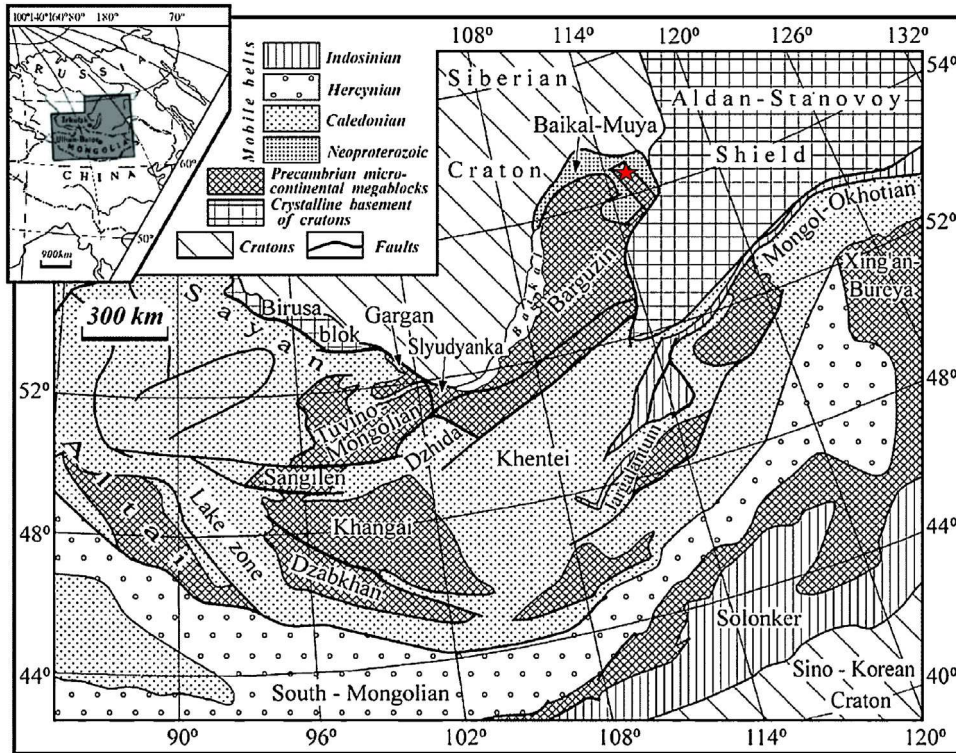


Fig. 1. Simplified tectonic division of the central Asia ([Kovalenko et al., 2004](#)). Star indicates the position of the North Muya eclogite–gneiss complex.

Sm–Nd geochronology for eclogites and their host gneisses in the North Muya block indicated that the age of high-pressure metamorphism (630 Ma) is significantly younger than U–Pb age of zircons from gneiss-granites ([Rytsk et al., 2007](#)), which are host rocks for eclogites and other high-pressure lithologies ([Shatsky et al., 1996, 2012](#)). However, there is no agreement among researchers regarding the closure temperature of the Sm–Nd system ([Mezger et al., 1992; Kylander-Clark et al., 2007](#)). From the available data, it is difficult to conclude whether the obtained mineral Sm–Nd age reflects the thermal peak of metamorphism or the timing of exhumation of high-pressure rocks. Taking into account the age of gneiss-granites, the question whether the eclogites and the host rocks were isofacial or were tectonically juxtaposed during the exhumation is still open. The host rocks do not demonstrate any features of high-pressure (HP) metamorphism. According to [Avchenko et al. \(1988\)](#), the peak metamorphic stage involved conditions of 650 °C and 9–10 kbars, while pressure estimates for eclogites are higher than 15 kbars and those for kyanite-bearing eclogite exceed 24 kbars ([Shatsky et al., 2012](#)).

To resolve this question, U–Pb dating of zircons from the country rocks of eclogite-bearing complex of North Muya dome is of crucial importance. The closure temperature of the U–Pb system is high in zircon; therefore, it can retain information about both the timing of HP metamorphism peak and age of the protoliths ([Rubatto and Hermann, 2007](#)). In addition, due to their low Lu/Hf value the calculated initial $^{176}\text{Hf}/^{177}\text{Hf}$ of zircons is relatively insensitive to age and close to the $^{176}\text{Hf}/^{177}\text{Hf}$ value of their parental melt. Combined U–Pb dating and Hf isotope information makes zircon an important tracer of mantle–crust evolution and interaction ([Scherer et al., 2007](#)).

U–Pb dating, Hf-isotope analyses on zircon and whole-rock Nd isotopes analyses were carried out for country rocks of the eclogite–gneiss complex of the North Muya dome.

2. Geological background

As have been mentioned above the Muya dome is situated in the Anamakit-Muya zone of the Baikal Muya accretionary fold belt (BMB) within the Baikalian orogen ([Rytsk et al., 2007, 2011](#)).

The North Muya dome has a heterogeneous structure (Fig. 2). Until now, the Muya dome has been interpreted to consist of several Archean rock units. It contains Early Archean (Dzhaltuk and Osinovka series), Late Archean (Tastakh unit), and Early Proterozoic (Parama series) rocks ([Avchenko et al., 1988](#)). The Early and Late Archean rocks form a series of tectonic blocks. Eclogites occur among the Early Archean gneisses of the Dzhaltuk and Osinovka series ([Avchenko et al., 1988](#)). Dzhaltuk series consisting of two mica gneisses, marbles and amphibolites. Osinovka series consisting of amphibolites and biotite-amphibol plagiogneisses. Most of the eclogite outcrops are confined to the tectonic contact between the Dzhaltuk and Tastakh units in a belt 10 km wide and 30 km long ([Dobretsov et al., 1989](#)). Eclogites occur as boudins or sheet-like bodies.

The granitic gneisses of the Ileir complex of the North Muya block has been dated at 786 ± 9 Ma (TIMS, U–Pb dating), raising some doubts about the Archean age of the rocks in the North Muya dome ([Rytsk et al., 2001](#)). However, geochronological data obtained by [Rytsk et al. \(2007, 2011\)](#) confirm the Riphean age of the metamorphic units in the “basement” of Baikal Muya Belt.

So far, there are different views regarding the age and geodynamic evolution of the North Muya dome. According to [Tsygankov \(2005\)](#), the Muya block is an allochthonous sialic block involved in the Late Riphean folding.

[Rytsk et al. \(2007, 2011\)](#) regarded the Anamakit-Muya zone of the Baikal-Muya belt as a continental-margin zone related to an outer subduction zone. According to this model, the Precambrian terrains are fragments of the Rodinia supercontinent, produced during continental rifting. A significant proportion of

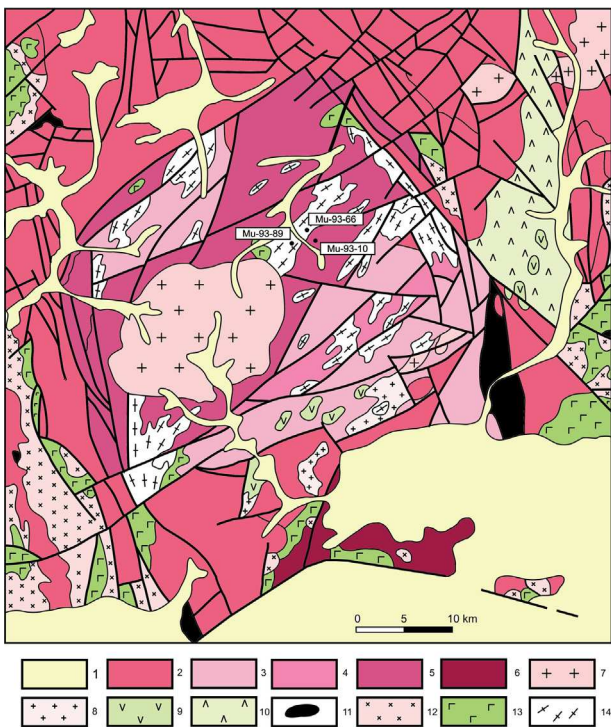


Fig. 2. Geological map of North Muya dome (Dobretsov et al., 1989). Solid circles indicate places of sampling. (1) Quaternary deposits; (2) Paleoproterozoic series; (3) Neoarchean series; (4–6) Mesoarchean series; (4) amphibolites and biotite-amphibole plagiogneisses of Osinovka unit; (5) two-mica gneisses with kyanite and marbles of Dzhaltuk series; (6) gneisses of Ust-Muya unit; (7–14) magmatic rocks: (7) Neoproterozoic granitoids; (8) granitoids of unknown age; (9) Neoproterozoic gabbroids; (10) granitoids of Vitim complex; (11) Paleoproterozoic ultrabasites; (12) Paleoproterozoic plagiogranites and granodiorites; (13) Paleoproterozoic gabbro and gabbro-diorites; (14) granitic gneisses of the Ileir complex.

the Anamakit-Muya zone, including the North Muya dome, was produced predominantly by reworking of the Early Precambrian crust with a subordinate contribution from juvenile sources. Neodymium-isotope compositions ($\varepsilon_{\text{Nd}}(t)$ from -17.6 to $+7.1$) provided the first evidence for mixing of juvenile and older crustal material (Rytsk et al., 2001, 2007, 2011; Kröner et al., 2014). According to Rytsk et al. (2001, 2007), separated shelf blocks collided between 0.8 and 0.78 Ma to produce the Baikal-Muya terrane with reworked ancient crust in the basement. The authors related the Late Baikalian rifting to the break-up of Rodinia and opening of the Paleoasian ocean.

Zorin et al. (2009) regarded the Muya dome as a block of Early Precambrian rocks in the Late Riphean island-arc zone, suggesting it might have been the basement of one of the island arcs. The age of the island-arc assemblages in the Baikal Muya belt is estimated to fall within the 825–700 Ma time interval. The Tallain gabbro-granite unit has an age of 612 ± 62 Ma and formed either at a final stage of the island-arc evolution or during the collisional magmatism. Zorin et al. (2009) suggested that the Late Riphean–Early Vendian collision caused only deformation of the island arc.

It should be noted that none of this model do not take into account the stage of continental collision evidenced by the eclogite-gneiss complex (Shatsky et al., 2012; Shatskii et al., 2014).

3. Samples and analytical methods

Zircons in this study were recovered from two granitic gneisses (Mu-93-89, Mu-93-66) and garnet-bearing two-mica schist (Mu-93-10). Major and trace element compositions of these samples have been published earlier (Shatsky et al., 2012).

Granitic gneisses consist of quartz, K-feldspar, plagioclase, biotite and garnet. The two-mica schist sample Mu-93-10 consists of Bt + Mu + Pl + Kfsp + Grt + Qtz. Apatite and allanite are accessory minerals.

In situ U-Pb and Hf-isotope analyses of zircons from country rocks were carried out in the Geochemical Analysis Unit of the GEMOC Key Center at the Department of Earth and Planetary Sciences, Macquarie University. Zircons were dated using the LA-ICP-MS technique. Hf-in-zircon isotopic analyses were performed using MC-LA-ICP-MS. Analytical procedures are given by Belousova et al. (2009). To calculate model ages (T_{DM}) based on a depleted-mantle source, we have adopted a model with $(^{176}\text{Hf}/^{177}\text{Hf})_i = 0.279718$ at 4.56 Ga and $^{176}\text{Lu}/^{177}\text{Hf} = 0.0384$; this produces a present-day value of $^{176}\text{Hf}/^{177}\text{Hf}$ (0.28325), similar to that of average MORB (Griffin et al., 2000, 2004). T_{DM} ages, which are calculated using the measured $^{176}\text{Lu}/^{177}\text{Hf}$ of the zircon, can only give a minimum age for the source material of the magma from which the zircon crystallized. Therefore we have also calculated, for each zircon, a “crustal” model age T_{DM}^{C} , which assumes that its parental magma was produced from an average continental crust ($^{176}\text{Lu}/^{177}\text{Hf} = 0.015$) that was derived from a depleted mantle.

Determinations of whole-rock Nd isotope compositions were carried out in laboratory of isotope geochemistry of the Institute of Geochemistry, Siberian Branch, Russian Academy of Sciences, using the multicollector thermoionizing FINNIGAN MAT 262 mass spectrometer of the Baikal Analytical Center SB RAS. The average value of the measured Nd isotope composition of the standard sample JNd-1 ($N=25$) $^{143}\text{Nd}/^{144}\text{Nd}$ amounted to 0.512109 ± 12 (2SE) at a recommended value of $^{143}\text{Nd}/^{144}\text{Nd}$ equal to 0.512110. The Nd model age are based the depleted mantle model of Michard et al. (1985).

4. Results

4.1. Zircon U-Pb dating and Hf-isotope composition

Zircons from garnet-biotite gneisses Mu-93-89 are mostly long prismatic crystals with ratios of length/width ranging from 2:1 to 3:1. CL imaging reveals that most grains have clear core–rim structure. The primary growth zoning is well preserved in some of the cores, whereas in others it is largely obliterated (Fig. 3a–c). The zircon morphology together with the well-developed oscillatory zoning as seen in CL images clearly identifies the magmatic origin of these grains. The rims exhibit no zoning or cloudy zoning typical of metamorphic zircons. Neoproterozoic U-Pb ages ranging from 630 to 792 Ma, were obtained for zircons from this sample (Table 1 , Figs. 3a–c and 4a). For the age data above 750 Ma the weighted averages age is 7645 ± 5.3 Ma (Fig. 4b). This age is consistent to the age of granite-gneisses of the Ileir complex (784 ± 5.9 Ma) (Rytsk et al., 2001, 2007, 2011). Three grains yield younger concordant ages (630–660 Ma) (Table 1 and Fig. 4a). Zircons have Th/U ratios scattering from 0.022 to 0.574. The lower Th/U ratios (0.007–0.271) are common to a younger zircon population with 639 ± 29 Ma age. These grains display no zoning or the cloudy zoning typical of metamorphic zircons (Fig. 3c). The absent or patchy zoning suggest that these zircons grew during a metamorphic event.

Most zircons from the Mu-93-66 granitic gneiss (length/width – 1:2 to 1:4.5) show either no zoning or patchy zoning in their CL images (Fig. 3d–f). Some grains have a core with relatively bright luminescence and oscillatory zoning rimmed by a darker zone. The zircons from this sample define concordant ages ranging from 576 to 866 Ma (Table 1 and Fig. 4c). Zircons with ages scattering from 708 to 771 exhibit a core with oscillatory zoning (Fig. 3d) that is interpreted to reflect crystallization from a melt. For the age data above 738 Ma the weighted averages age is 763 ± 14 (Fig. 4d). One zircon grain gave a concordant age of 866 ± 9 Ma (Fig. 4c). Grains

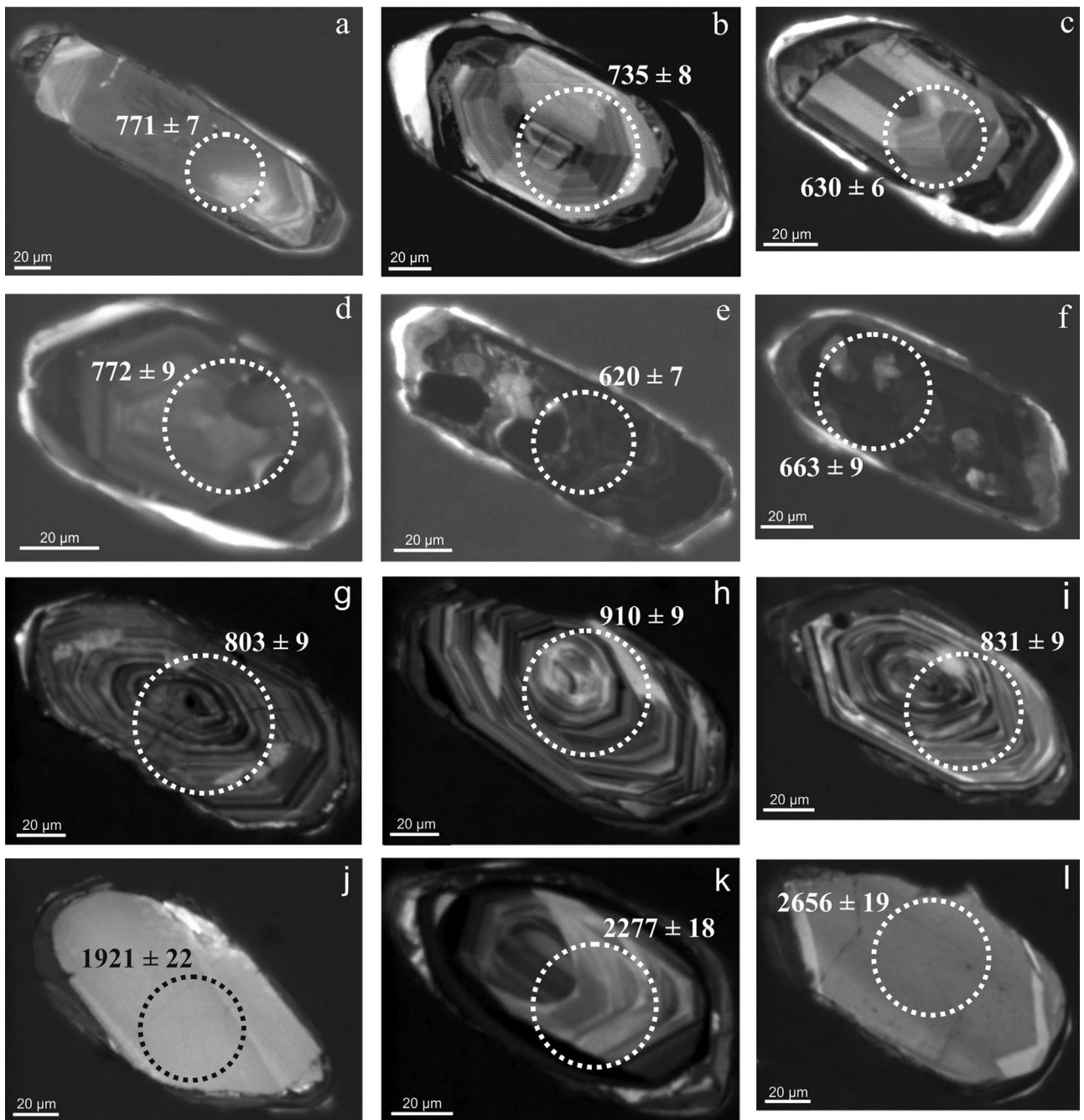


Fig. 3. CL images for zircons from granite-gneisses Mu-93-89 (a–c), Mu-93-66 (d–f) and a two-mica schist Mu-93-10 (g–l). Labeled ages are $^{207}\text{Pb}/^{206}\text{Pb}$ ages for zircons older than 1.0 Ga and $^{206}\text{Pb}/^{238}\text{U}$ ages for zircons younger than 1.0 Ga. Numbers within crystals denote analytically concordant $^{206}\text{Pb}/^{238}\text{U}$ ages. Locations of U–Pb isotope analytical spots are shown by dashed circles.

from old population have Th/U ratios varying from 0.163 to 0.779, while younger (576–680 Ma) zircons show significantly lower Th/U ratios (0.0004–0.021). In the granitic gneiss Mu-93-66 five grains of zircons give an age roughly consistent (610–663 Ma) to the Sm–Nd internal isochron ages for the eclogites (631 ± 17) and host gneiss (636 ± 9) (Shatsky et al., 2012).

The two-mica schist Mu-93-10 contains two populations of zircons. Weakly colored zircons with width/length ratios of 1.6–3.4 demonstrate a clear oscillatory zoning (Fig. 3g–i). Concordant ages of these zircons range from 793 to 941 Ma (Table 1 and Fig. 4e).

Zircons from the second population are light brown with rounded detrital cores. Primary growth zoning is well preserved in some of the cores, whereas in others it is largely obliterated (Fig. 3j–l). Nine analyses of inherited cores gave $^{207}\text{Pb}/^{206}\text{Pb}$ ages between 3238 ± 23 and 1882 ± 23 (Table 1 and Fig. 4g). Zircons with these ages have the highest (3.04) and the lowest (0.05) Th/U values (Table 1). The lowest Th/U ratio is found in the oldest grain (3.2 Ga). This low Th/U value is interpreted as an evidence of a metamorphic origin (Rubatto and Hermann, 2007). As opposed to zircons from other samples, most grains in a younger population from the

sample Mu-93-10 exhibit clear oscillatory zoning and thin outer rims.

Lu/Hf ratios of zircons from gneisses and schist vary in a range (from 0.0002 to 0.0003) (**Table 2**). There is a wide spread in their $^{176}\text{Hf}/^{177}\text{Hf}_\text{i}$ ratios (0.28270–0.28092), $\varepsilon_{\text{Hf}}(t)$ (−15.3 to +13.9), as well as in T_{DM} (0.77–3.18) and T_{DM}^{C} (0.82–3.86) model ages. The two-mica schist Mu-93-10 has the widest scatter of these values $\varepsilon_{\text{Hf}}(t)$ from +13.9 to −15.3, T_{DM} (0.82–3.18 Ga),

T_{DM}^{C} (0.82–3.86 Ga). Other samples have a much narrower range ($\varepsilon_{\text{Hf}}(t)$ +11.6 to −0.7), T_{DM} (0.73–1.23 Ga) and T_{DM}^{C} (0.85–1.52 Ga).

4.2. Whole-rock Nd isotopes

Nd-isotope compositions of nine country-rock and four eclogite samples are given in **Table 3**. We have reported

Table 1
U–Pb–Th-age data for North Muya rocks.

Sample	^{232}Th (ppm)	^{238}U (ppm)	Th/U	Isotoperatios								
				$^{207}\text{Pb}/^{206}\text{Pb}$	1σ	$^{207}\text{Pb}/^{235}\text{U}$	1σ	$^{206}\text{Pb}/^{238}\text{U}$	1σ	$^{208}\text{Pb}/^{232}\text{Th}$	1σ	
Mu-93-89	9	185,411	695,432	0.267	0.06473	0.00076	1.12542	0.01418	0.12610	0.00144	0.03590	0.00060
	12	55,790	508,930	0.110	0.06402	0.00099	1.06713	0.01689	0.12090	0.00145	0.03949	0.00113
	13	40,150	252,280	0.159	0.06350	0.00092	1.04087	0.01570	0.11890	0.00143	0.04187	0.00091
	35	101,303	729,253	0.139	0.06364	0.00069	1.05940	0.01219	0.12075	0.00132	0.03709	0.00051
	37	138,638	511,238	0.271	0.06215	0.00090	0.91436	0.01248	0.10671	0.00108	0.03348	0.00077
	38	242,007	552,897	0.438	0.06507	0.00086	1.12487	0.01585	0.12539	0.00151	0.03734	0.00070
	39	179,389	530,485	0.338	0.06740	0.00081	1.17274	0.01526	0.12620	0.00148	0.03837	0.00061
	40	150,199	1,960,807	0.077	0.06216	0.00071	0.88008	0.00990	0.10270	0.00104	0.03272	0.00059
	41	150,780	549,213	0.275	0.06458	0.00072	1.10748	0.01282	0.12439	0.00134	0.03741	0.00054
	44	157,140	679,889	0.231	0.06559	0.00093	1.14429	0.01698	0.12654	0.00152	0.03717	0.00090
	47	32,515	1,449,138	0.022	0.06176	0.00074	0.91292	0.01138	0.10722	0.00120	0.04328	0.00097
	58	247,091	430,208	0.574	0.06495	0.00072	1.13807	0.01255	0.12710	0.00130	0.03820	0.00049
	58-1	156,900	426,752	0.368	0.06388	0.00089	1.07418	0.01576	0.12197	0.00148	0.03496	0.00069
	64	89,693	311,671	0.288	0.06352	0.00112	1.02984	0.01748	0.11760	0.00132	0.04225	0.00120
	66	14,019	1,766,257	0.008	0.06308	0.00074	0.87338	0.01118	0.10043	0.00118	0.07466	0.00183
	68	128,764	688,581	0.187	0.06567	0.00080	1.12895	0.01461	0.12468	0.00144	0.03634	0.00067
	70	76,984	525,201	0.147	0.06582	0.00101	1.18545	0.01894	0.13064	0.00161	0.03663	0.00103
	100	143,315	504,239	0.284	0.06320	0.00133	1.01485	0.02017	0.11646	0.00130	0.03382	0.00151
	105	99,300	497,523	0.200	0.06510	0.00087	1.14202	0.01586	0.12724	0.00146	0.03639	0.00080
	108	170,563	454,199	0.376	0.06444	0.00082	1.11267	0.01499	0.12526	0.00145	0.03499	0.00067
	29	373,536	655,832	0.570	0.06618	0.00085	1.21044	0.01638	0.13268	0.00154	0.03932	0.00079
	32	250,911	426,536	0.588	0.06927	0.00073	1.44719	0.01582	0.15153	0.00160	0.04528	0.00051
	33	150,635	386,628	0.390	0.14407	0.00150	8.34262	0.09064	0.42001	0.00448	0.11248	0.00132
	38	345,127	732,508	0.471	0.06854	0.00081	1.36350	0.01562	0.14427	0.00145	0.04438	0.00076
	41	235,037	409,916	0.573	0.06684	0.00085	1.25426	0.01699	0.13613	0.00161	0.04029	0.00067
	44	221,620	432,352	0.513	0.06805	0.00092	1.32429	0.01760	0.14113	0.00151	0.04372	0.00093
	45	157,144	395,305	0.398	0.13187	0.00147	6.45920	0.07825	0.35530	0.00406	0.09897	0.00158
	48	76,129	188,798	0.403	0.18032	0.00208	12.46861	0.14736	0.50153	0.00544	0.13971	0.00250
	72	169,397	486,746	0.348	0.13869	0.00185	7.21505	0.10241	0.37739	0.00456	0.10587	0.00270
	93	179,302	374,499	0.479	0.06650	0.00110	1.22408	0.01910	0.13352	0.00139	0.04385	0.00131
Mu-93-10	96	276,929	502,470	0.551	0.06633	0.00107	1.25801	0.02022	0.13757	0.00160	0.04213	0.00119
	98	391,888	128,734	3.044	0.11765	0.00145	5.69023	0.07379	0.35085	0.00406	0.09861	0.00166
	101	869,230	1,675,237	0.519	0.13889	0.00156	6.86004	0.08205	0.35831	0.00400	0.10401	0.00183
	117	1,450,051	975,305	1.487	0.06696	0.00103	1.30889	0.02112	0.14177	0.00177	0.04168	0.00120
	121	347,609	430,687	0.807	0.06628	0.00085	1.24617	0.01701	0.13639	0.00162	0.03892	0.00065
	124	310,206	649,037	0.478	0.06561	0.00085	1.18427	0.01642	0.13091	0.00156	0.03808	0.00075
	128	308,728	1,244,942	0.248	0.06563	0.00071	1.18803	0.01336	0.13130	0.00141	0.04086	0.00056
	131	50,051	1,060,032	0.047	0.25854	0.00375	21.01134	0.30844	0.58953	0.00668	0.14398	0.00468
	135	201,140	285,995	0.703	0.11489	0.00143	5.38273	0.07185	0.33984	0.00403	0.09006	0.00184
	137	342,825	495,850	0.691	0.06998	0.00087	1.51557	0.02010	0.15709	0.00184	0.04460	0.00080
	139	800,325	1,031,125	0.776	0.11514	0.00146	5.33061	0.07290	0.33582	0.00401	0.09515	0.00221
	1	13,797	969,529	0.014	0.06048	0.00145	0.83583	0.02004	0.10022	0.00152	0.04340	0.00270
	5	8571	975,043	0.009	0.05723	0.00176	0.78841	0.02393	0.09989	0.00169	0.03523	0.00321
	6	6103	1,331,106	0.005	0.06065	0.00089	0.84461	0.01240	0.10102	0.00113	0.03357	0.00177
	24	7743	1,684,497	0.005	0.06047	0.00100	0.82782	0.01412	0.09931	0.00124	0.04443	0.00241
	22	64,249	120,140	0.535	0.06481	0.00198	1.13104	0.03374	0.12659	0.00196	0.03656	0.00178
	35	64,882	242,421	0.268	0.06431	0.00103	1.07506	0.01639	0.12128	0.00128	0.04199	0.00122
	44	198,091	775,366	0.255	0.06353	0.00093	1.08490	0.01665	0.12384	0.00150	0.03837	0.00106
	45	230,413	513,132	0.449	0.06700	0.00081	1.32836	0.01671	0.14381	0.00159	0.04414	0.00079
	58	156,032	753,154	0.207	0.06407	0.00088	0.97230	0.01313	0.11009	0.00117	0.03887	0.00099
	61	9671	1,608,122	0.006	0.05901	0.00114	0.75996	0.01504	0.09340	0.00126	0.05322	0.00346
Mu-93-66	66	42,138	258,711	0.163	0.06293	0.00180	1.00848	0.02793	0.11625	0.00170	0.02736	0.00175
	75	143,923	408,758	0.352	0.06438	0.00093	1.12968	0.01694	0.12729	0.00152	0.03652	0.00091
	81	23,851	1,809,408	0.013	0.06309	0.00113	0.80998	0.01480	0.09313	0.00120	0.07858	0.00345
	82	5368	1,353,580	0.004	0.06070	0.00114	0.87025	0.01665	0.10400	0.00137	0.06170	0.00436
	84	1,207,741	1,550,772	0.779	0.06500	0.00113	1.13667	0.02026	0.12684	0.00162	0.03581	0.00138
	85	8567	1,900,380	0.005	0.06105	0.00099	0.85159	0.01388	0.10124	0.00120	0.06796	0.00355
	88	232,333	1,125,424	0.206	0.06314	0.00097	1.02534	0.01646	0.11779	0.00144	0.03860	0.00121
	94	5384	682,054	0.008	0.06233	0.00162	0.93098	0.02342	0.10837	0.00151	0.08557	0.00738
	96	159,512	457,014	0.349	0.06475	0.00204	1.09477	0.03373	0.12267	0.00208	0.02007	0.00118
	97	21,434	3,815,553	0.006	0.06335	0.00070	0.80444	0.00941	0.09211	0.00101	0.09924	0.00185
	99	12,193	578,746	0.021	0.06232	0.00111	0.95502	0.01685	0.11121	0.00133	0.08392	0.00379

Table 1 (Continued)

Sample	Ages (Ma)								Concordance	
	$^{207}\text{Pb}/^{206}\text{Pb}$	1 σ	$^{207}\text{Pb}/^{235}\text{U}$	1 σ	$^{206}\text{Pb}/^{238}\text{U}$	1 σ	$^{208}\text{Pb}/^{232}\text{Th}$	1 σ		
Mu-93-89	9	766	25	713	7	766	8	713	12	100
	12	742	32	783	8	736	8	783	22	99
	13	725	30	829	8	724	8	829	18	100
	35	730	23	734	6	735	8	736	10	100
	37	679	31	659	7	654	6	666	15	96
	38	777	27	765	8	762	9	741	14	98
	39	850	25	788	7	766	8	761	12	90
	40	680	24	641	5	630	6	651	12	93
	41	761	23	757	6	756	8	742	10	99
	44	793	29	775	8	768	9	738	18	97
	47	666	25	659	6	657	7	856	19	99
	58	773	23	758	6	771	7	758	10	100
	58-1	738	29	695	8	742	8	695	13	100
	64	726	37	836	9	717	8	836	23	99
	66	711	25	1455	6	617	7	1455	34	87
	68	796	25	767	7	758	8	722	13	95
	70	801	32	794	9	792	9	727	20	99
	100	715	44	672	10	710	8	672	30	99
	105	778	28	723	8	772	8	723	16	99
	108	756	27	695	7	761	8	695	13	100
Mu-93-10	29	812	27	805	8	803	9	779	15	99
	32	907	22	909	7	910	9	895	10	100
	33	2277	18	2269	10	2261	20	2155	24	99
	38	885	24	873	7	869	8	878	15	98
	41	833	26	825	8	823	9	798	13	99
	44	870	28	856	8	851	9	865	18	98
	45	2123	19	2040	11	1960	19	1908	29	92
	48	2656	19	2640	11	2620	23	2643	44	99
	72	2211	23	2138	13	2064	21	2034	49	93
	93	822	34	812	9	808	8	868	25	98
	96	817	33	827	9	831	9	834	23	100
	98	1921	22	1930	11	1939	19	1901	31	100
	101	2213	19	2094	11	1974	19	2000	34	89
	117	837	32	850	9	855	10	825	23	100
	121	815	26	822	8	824	9	772	13	100
	124	794	27	793	8	793	9	755	15	100
	128	795	22	795	6	795	8	810	11	100
	131	3238	23	3139	14	2988	27	2719	83	92
	135	1878	22	1882	11	1886	19	1743	34	100
	137	928	25	937	8	941	10	882	16	100
	139	1882	23	1874	12	1867	19	1837	41	99
Mu-93-66	1	621	51	617	11	616	9	859	52	100
	5	500	67	590	14	614	10	700	63	100
	6	627	31	622	7	620	7	667	35	99
	24	620	35	612	8	610	7	879	47	98
	22	768	63	768	16	768	11	726	35	100
	35	752	33	741	8	738	7	831	24	98
	44	726	31	746	8	753	9	761	21	100
	45	838	25	858	7	866	9	873	15	100
	58	744	29	690	7	673	7	771	19	91
	61	568	41	574	9	576	7	1048	66	100
	66	706	60	708	14	709	10	546	35	100
	75	754	30	768	8	772	9	725	18	100
	81	711	38	602	8	574	7	1529	65	81
	82	629	40	636	9	638	8	1210	83	100
	84	774	36	771	10	770	9	711	27	99
	85	641	34	626	8	622	7	1329	67	97
	88	713	32	717	8	718	8	766	23	100
	94	686	55	668	12	663	9	1660	137	97
	96	766	65	751	16	746	12	402	23	97
	97	720	23	599	5	568	6	1913	34	79
	99	685	38	681	9	680	8	1629	71	99

petrography and chemical compositions of these samples previously ([Shatsky et al., 2012](#)). The gneisses and schists exhibit a range of Nd isotopic composition with $\varepsilon_{\text{Nd}}(t)$ values ranging from -3.54 to +3.57 and $t_{\text{Nd(DM)}}$ from 1.61 to 1.05 Ga. Eclogites have $\varepsilon_{\text{Nd}}(t)$ of +0.32 to +6.9 and $t_{\text{Nd(DM)}}$ of 1.6–0.72.

5. Discussion

5.1. Isotopic evidence of crustal reworking

The obtained data indicate several tectonothermal events in the evolution of the eclogite-bearing complex of the North Muya dome.

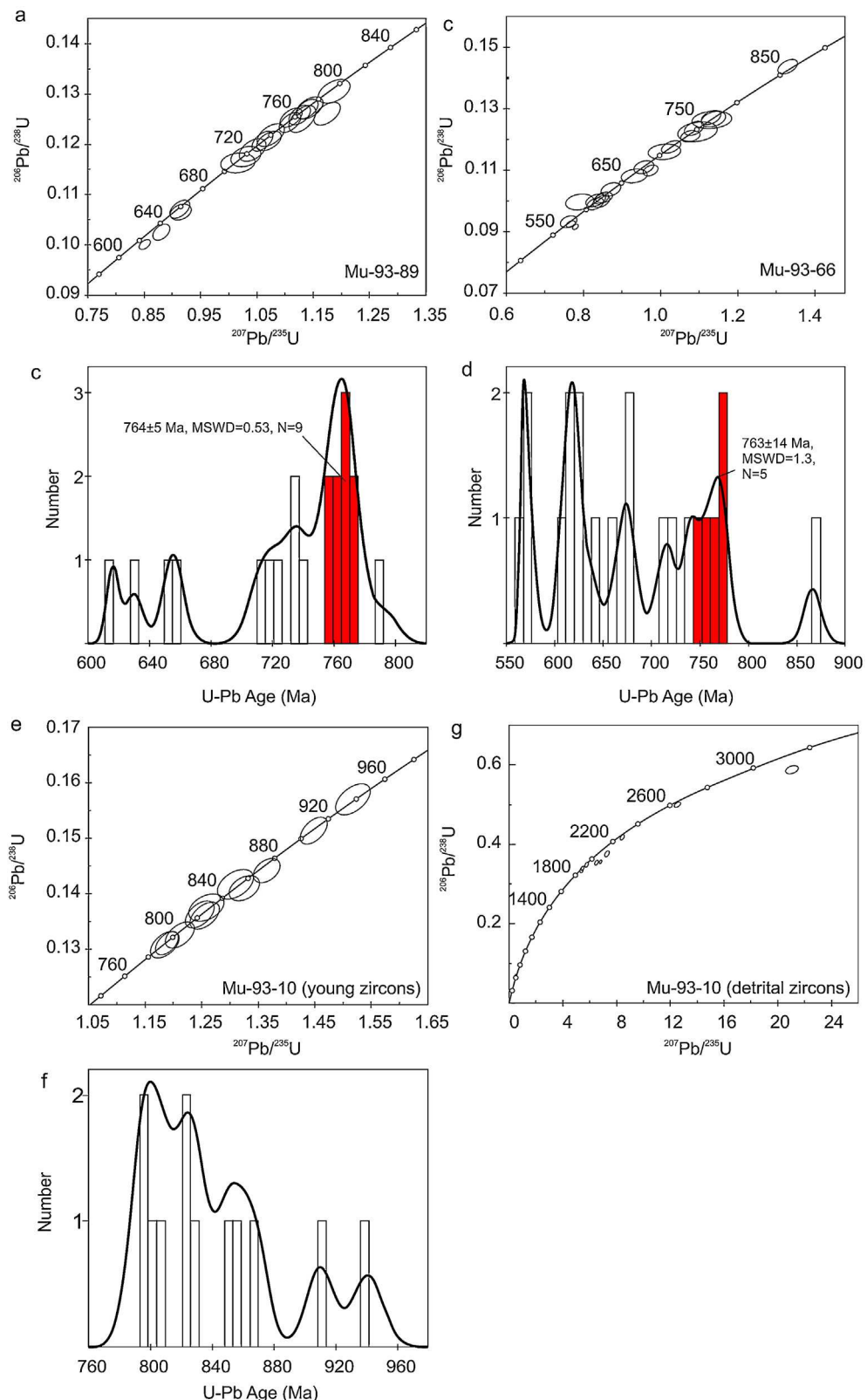


Fig. 4. Concordia diagrams and relative probability plot for LA-ICPMS data for zircons from granite-gneisses Mu 93-89 (a and b), Mu 93-66 (c and d) and a two-mica schist Mu 93-10 (e and f – young generation, g – detrital zircons).

Zircons from granitic gneisses Mu-93-66 and Mu-93-89 yielded U-Pb ages (Fig. 4) broadly similar to the age of granitic gneisses of the Ileir complex. Note that all grains from those samples except for three zircon yield an age less than 800 Ma. The positive $\varepsilon_{\text{Hf}}(t)$

values and the Mesoproterozoic model Hf age (T_{DM}^{C}) (1.13–1.52 Ga) of the zircons with oscillatory zoning suggest the dominance of the juvenile component in the protolith of the granitic gneisses.

Table 2

Lu-Hf isotope data for zircons from metamorphic rocks of North Muya dome.

Sample		$^{176}\text{Hf}/^{177}\text{Hf}$	1σ	$^{176}\text{Lu}/^{177}\text{Hf}$	$^{176}\text{Yb}/^{177}\text{Hf}$	U/Pb age (Ma)	Hf _f	ε_{Hf}	1σ	T_{DM} (Ga)	$T_{\text{DM}}^{\text{Crustal}}$ (Ga)
	29	0.282043	0.000014	0.000940	0.034543	803	0.282029	-8.8	0.5	1.70	2.14
	32	0.282474	0.000011	0.001191	0.040172	910	0.282454	8.6	0.4	1.11	1.20
	33	0.281187	0.000013	0.000440	0.018751	2277	0.281168	-5.7	0.5	2.84	3.15
	38	0.282372	0.000017	0.001412	0.050263	869	0.282349	4.0	0.6	1.26	1.45
	41	0.282581	0.000011	0.001221	0.036681	823	0.282562	10.5	0.4	0.96	1.02
	44	0.282412	0.000028	0.001362	0.036020	851	0.282390	5.1	1.0	1.20	1.37
	45	0.281447	0.000019	0.000479	0.016711	2123	0.281428	0.0	0.7	2.49	2.70
	48	0.281012	0.000015	0.001017	0.044168	2656	0.280960	-4.2	0.5	3.12	3.37
	72	0.281486	0.000019	0.000909	0.031770	2211	0.281448	2.7	0.7	2.47	2.60
	96	0.282548	0.000013	0.000713	0.021179	831	0.282537	9.8	0.5	0.99	1.07
Mu-93-10	98 core	0.280936	0.000022	0.000558	0.026951		0.280916	0.8	3.18	3.86	
	98 rim	0.281150	0.000032	0.000570	0.018685	1921	0.281129	-15.3	1.1	2.90	3.42
	101	0.281126	0.000019	0.000342	0.013250	2192	0.281112	-9.6	0.7	2.91	3.31
	117	0.282048	0.000025	0.002547	0.104989	855	0.282007	-8.4	0.9	1.77	2.16
	121	0.282690	0.000017	0.002186	0.080403	824	0.282656	13.9	0.6	0.82	0.82
	128	0.282443	0.000014	0.000561	0.021259	795	0.282435	5.4	0.5	1.13	1.31
	131	0.281001	0.000014	0.000515	0.019304	3238	0.280969	9.8	0.5	3.09	3.01
	135	0.281459	0.000020	0.000654	0.022421	1878	0.281436	-5.4	0.7	2.49	2.81
	137	0.282443	0.000013	0.001029	0.035841	941	0.282425	8.3	0.5	1.15	1.25
	139 core	0.281538	0.000031	0.000619	0.026545	1882	0.281516	-2.4	1.1	2.38	2.64
	139 rim	0.281918	0.000022	0.000337	0.010090	1882	0.281906	11.4	0.8	1.84	1.83
	1	0.282516	0.000019	0.000541	0.015991	616	0.282510	4.0	0.7	1.03	1.24
	22	0.282515	0.000010	0.000838	0.033235	768	0.282503	7.2	0.3	1.04	1.18
	35	0.282541	0.000012	0.000738	0.031951	738	0.282531	7.5	0.4	1.00	1.13
	44	0.282510	0.000011	0.000468	0.013907	753	0.282503	6.9	0.4	1.04	1.18
	45	0.282476	0.000012	0.000965	0.035410	866	0.282460	7.9	0.4	1.10	1.21
Mu-93-66	58	0.282517	0.000013	0.001320	0.046340	673	0.282500	4.9	0.5	1.05	1.23
	61	0.282518	0.000016	0.000179	0.009727	576	0.282516	3.3	0.6	1.02	1.25
	75	0.282524	0.000013	0.000767	0.033722	772	0.282513	7.6	0.5	1.02	1.15
	82	0.282479	0.000017	0.000474	0.014561	638	0.282473	3.2	0.6	1.08	1.31
	84	0.282472	0.000012	0.000796	0.024555	770	0.282460	5.7	0.4	1.10	1.26
	85	0.282376	0.000012	0.000208	0.006745	622	0.282374	-0.7	0.4	1.21	1.52
	88	0.282490	0.000012	0.000386	0.014933	718	0.282485	5.4	0.4	1.06	1.24
	47	0.282457	0.000014	0.001788	0.072910	657	0.282435	2.3	0.5	1.15	1.38
	58	0.282419	0.000011	0.001396	0.054113	771	0.282399	3.6	0.4	1.19	1.39
	58-1	0.282453	0.000011	0.001630	0.067212	742	0.282430	4.0	0.4	1.15	1.34
	64	0.282432	0.000013	0.001313	0.054452	717	0.282414	2.9	0.5	1.17	1.39
Mu-93-89	66	0.282434	0.000013	0.000843	0.032315	616	0.282424	1.0	0.5	1.15	1.42
	68	0.282478	0.000015	0.002976	0.128571	757	0.282436	4.5	0.5	1.16	1.32
	70	0.282424	0.000025	0.001875	0.074030	792	0.282396	3.9	0.9	1.20	1.39
	100	0.282456	0.000009	0.001222	0.051093	710	0.282440	3.6	0.3	1.13	1.34
	105	0.282417	0.000024	0.002631	0.092384	772	0.282379	2.9	0.8	1.23	1.43
	108	0.282443	0.000012	0.001401	0.057581	761	0.282423	4.2	0.4	1.16	1.35

Ages of the part of metamorphic zircons from the country rocks are roughly consistent with the Sm–Nd mineral isochron of eclogites (631 ± 17 Ma) (Shatsky et al., 2012) and provide with convincing evidences that their protoliths underwent a simultaneous high-pressure metamorphism. A number of zircons from the sample Mu-93-66 gave an age ranging from 575 to 620 Ma. It is probably the age of exhumation of rocks or the final collision stage.

Zircons from the two-mica schist Mu-93-10 show the greatest scatter in U–Pb ages. In addition to the Neoproterozoic grains with oscillatory zoning (800–940 Ma), this sample also contains detrital zircons with Paleoproterozoic (7 grains) and Archean (2 grains) cores (Fig. 4).

The Neoproterozoic zircons from the garnet–biotite gneisses exhibit magmatic zoning; the large scatter of $\varepsilon_{\text{Hf}}(t)$ values (-0.7

Table 3
Sm–Nd isotope data for North Muya rocks.

Sample	Nd (ppm)	Sm (ppm)	$^{147}\text{Sm}/^{144}\text{Nd}$	$^{143}\text{Nd}/^{144}\text{Nd}$	\pm	ε_{Nd}	$\varepsilon_{\text{Nd}}(t)$	$T_{\text{Nd}}(\text{DM})$	$T_{\text{Nd}}(\text{DM-2ST})$
Mu-93-55	15.5	4.90	0.1913	0.512969	16	6.46	6.90	0.72	
Mu-93-73	22	6.1	0.1669	0.512588	5	-0.98	1.77	1.45	
Mu-93-90	17	5.1	0.1806	0.512671	5	0.64	2.13	1.63	
Mu-93-93	167	37	0.1334	0.512343	6	-5.75	0.08	1.32	
Mu-93-3	4.9	1.28	0.1572	0.512295	6	-6.69	-3.06	1.92	1.59
Mu-93-10	23.5	4.3	0.1101	0.512079	13	-10.9	-2.94	1.41	1.58
Mu-93-19	47	11	0.1409	0.51232	6	-6.20	-1.07	1.49	1.43
Mu-93-44	73	17.5	0.1443	0.512292	5	-6.75	-1.93	1.61	1.50
Mu-93-45	61	15.9	0.1569	0.512625	4	-0.25	3.42	1.14	1.08
Mu-93-48	61	14.8	0.1460	0.512208	7	-8.39	-3.73	1.81	1.64
Mu-93-54	79.8	20.68	0.1567	0.512437	13	-3.92	-0.70	1.58	1.33
Mu-93-66	57	11.8	0.1246	0.512278	4	-7.02	-0.39	1.31	1.38
Mu-93-89	43	10.3	0.1442	0.512285	6	-6.89	-2.05	1.62	1.51

Mu-93-73, Mu-93-90, Mu-93-93, Mu-93-55 – eclogites; Mu-93-3, Mu-93-44, Mu-93-45, Mu-93-48 – two-mica schist; Mu-93-66, Mu-93-19, Mu-93-89, Mu-93-54 – granitic gneisses.

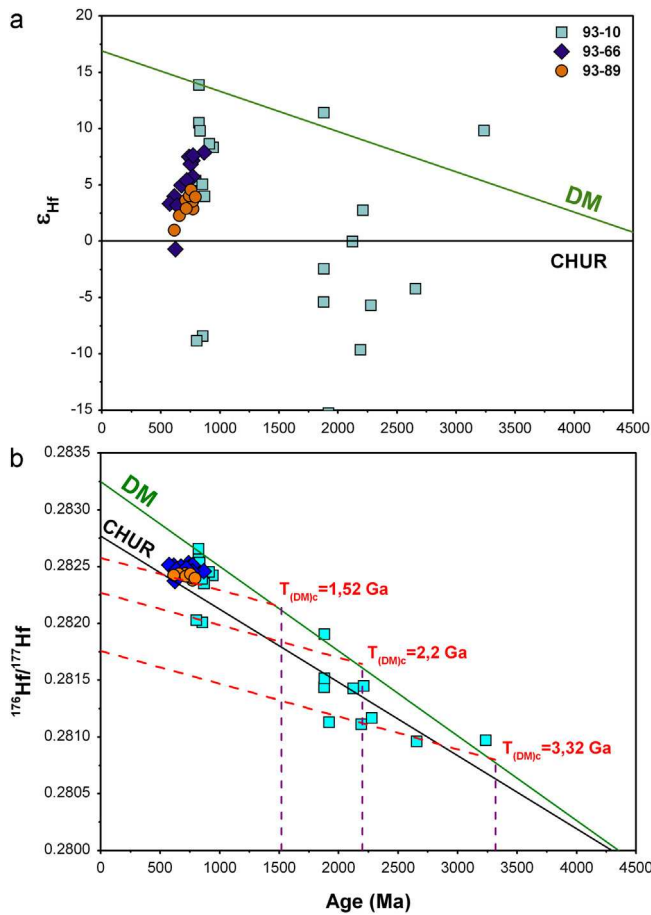


Fig. 5. Plots of U–Pb age versus $\epsilon_{\text{Hf}}(t)$ (a) and initial $^{176}\text{Hf}/^{177}\text{Hf}$ (b) for in situ Lu–Hf isotopic studies of zircons from gneisses and schists of Northern Muya HP metamorphic complex. Interpreted crustal evolution lines and their T_{DM}^{C} values shown for the major age clusters of data.

to +7.9) suggesting mixing of old continental crust with juvenile material (Table 2 and Fig. 5). It is clearly shown by the zircon from sample Mu-93-10 (grain 29) that yielded the U–Pb crystallization age of 803 Ma and a T_{DM}^{C} model age of 2.14 Ga, reflecting negative $\epsilon_{\text{Hf}}(t)$ values (−8.8) (Table 2). This grain also shows a thin oscillatory zoning, evidence of its crystallization from a melt. One zircon grain (121) shows a similar U–Pb age of crystallization and T_{DM}^{C} (Table 2 and Fig. 5). Grains older than 1.88 Ga show both positive and negative $\epsilon_{\text{Hf}}(t)$. The oldest grain (3.32 Ga) has an initial Hf-isotope ratio that corresponds to the depleted mantle value (Fig. 5). A number of inherited zircons gave T_{DM}^{C} Hf model ages of 3.32 Ga, assuming that the protolith of each magmatic rock had the $^{176}\text{Lu}/^{177}\text{Hf}$ of the mean continental crust (0.015).

Thus, the zircons of the two-mica schist sample Mu-93-10 record Paleoproterozoic (2.1 and 1.9 Ga) and Neoproterozoic (800–850 Ma) episodes during which the Archean crust remelted, producing magmas that mixed with juvenile material (Fig. 5 and Table 2).

A number of grains with detrital cores in sample Mu-93-10 suggest a metasedimentary protolith. The U–Pb ages and Hf-isotope compositions of the zircons from this sample suggest Paleoarchean and Paleoproterozoic sources. In the Neoproterozoic the metasedimentary rocks underwent reworking with some juvenile addition.

It should be stressed that the abundance of radiometric ages scattering from 2.0 to 1.8 Ga in the rocks of the Siberian craton may record the time of tectonic amalgamation (Rosen et al., 2006). The crustal growth event dated at 3.3 Ga has been observed widely

in the Aldan-Stanovoy Shield of the Siberian craton (Rosen et al., 2006). In whole-rock sample Mu-93-10 lacks Eu anomaly (Shatsky et al., 2012); negative Eu anomalies, reflecting crystallization of plagioclase, are a characteristic feature of the Proterozoic upper crust, but are rare in the Archean crust (Taylor and McLennan, 1995). All the above data suggest that clastic sediments are most likely a protolith of two-mica schist Mu-93-10. We believe that the source for those clastic metasediments was located on the Siberian craton. The 800–940 Ma tectonothermal event can be related to the break-up of Rodinia and opening of the Paleoasian ocean.

The gneisses and schist's exhibit a range of Nd isotopic composition with $\epsilon_{\text{Nd}}(t)$ values ranging from −5 to +3 and $t_{\text{Nd}(\text{DM})}$ from 1.89 to 1.13. Two-stage Nd model ages for samples Mu-93-66 (1.38 Ga) and Mu-93-89 (1.51 Ga) are close to the Hf T_{DM}^{C} . Nd model age for sample Mu-93-10 (1.6 Ga), which contains an Archean component, and is close to model ages for other samples. As stated above, the zircon studies indicate a multi-stage episodic reworking of the Archean crustal material. Thus, it is rather difficult to define which stage corresponds to the recent Sm–Nd value in this sample and there are uncertainties with regard to the model age. Based on isotopic data we conclude that Neoproterozoic gneisses and schist is characterized by reworking of Paleoproterozoic and Archean crust with additions of juvenile material.

Though zircons from other samples show the 650 Ma event that is close to the age of high-pressure metamorphism, the zircons from the sample Mu-93-10 do not reflect this event. The zircons showing the 750–770 Ma tectonic-thermal stage are also not evident in this sample though this stage is recorded in samples Mu-93-66 and Mu-93-89. It must be emphasized that the model age $T_{\text{Nd}(\text{DM})}$ of the not contaminated eclogite (720 Ma) roughly consistent with 750–770 tectonic-thermal stage (Shatsky et al., 2012). With this data we suggest that prior to the collision granitic gneisses and schist may have belonged to different blocks.

5.2. Tectonic interpretation

The available geochronological data (Shatsky et al., 2012; Shatskii et al., 2014) together with the results obtained from this study point out the coeval metamorphism of eclogites and at least part of their host rocks. Pressure estimates for the eclogite-facies metamorphism in the range from 15 to 25 kbars suggest that the protoliths of eclogites and rocks of the continental crust were subducted to depths corresponding to the upper mantle. Thus, the eclogite–gneiss complex of the North Muya dome reflects continental subduction (Ernst, 2001; Liou et al., 2009) in the Baikal Muya fold belt. The continental subduction followed the oceanic subduction; the early collision stage was responsible for the formation and exhumation of high-pressure metamorphic rocks (Song et al., 2006; Warren et al., 2008; Li et al., 2011; Burov et al., 2014).

Both lateral and vertical heterogeneities are obvious the geological-seismic profile of the Anamakit-Muya zone (Bulgatov, 1988). According to Bulgatov and Gordienko (1999) borders between high-velocity and low-velocity blocks are inclined eastward and could be either subduction or obduction planes (Bulgatov, 1988). The above researchers believe that the oceanic and island-arc terranes were subducted beneath the Muya cratonic terrane and the Chara-Olekma block of the Siberian craton.

Taking into account seismic data and that, according to our data eclogite-bearing complex the Muya dome represent a tectonic mélange comprising rocks of different blocks, we offer the following geodynamic model.

On the seismic profile the Muya block is shown as a heterogeneous body subducted eastwards beneath the Olekma granite–greenschist terrane of the Siberian craton (Fig. 6). The V_p wave velocities suggest that this body is composed of rocks similar to those exposed now in the North Muya dome (Bulgatov, 1988;

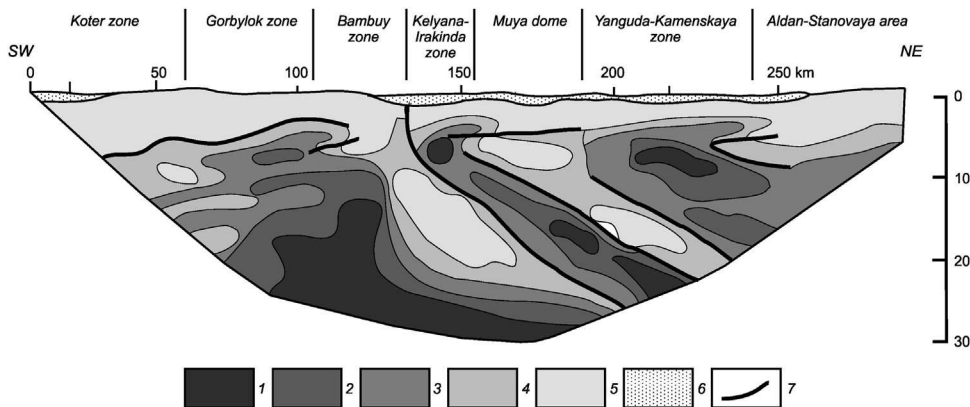


Fig. 6. Tectonic structure of Baikal-Muya fold belt. Seismic profile. Seismic waves velocity, km/s: (1) >6.6; (2) 6.6–6.4; (3) 6.4–6.2; (4) 6.2–6.0; (5) <6.0; (6) Baikal rift zone deposits; (7) faults (Tsygankov, 2005).

(Bulgatov and Gordienko, 1999). We suggest that an ensialic island arc containing fragments of continental basement was involved in the oceanic subduction zone beneath the margin of the Siberian craton. Thermo-mechanical and numerical modeling indicates that the involvement of a low-density block in the subduction initiated slab break off resulted in the exhumation of subducted continental crust due to its low density (Ernst, 2001; Burov et al., 2014). The rocks were exhumed from the depth corresponding to high-pressure (HP) and ultra-high pressure (UHP) metamorphism as thin blocks or mélange (Burov et al., 2014). During the exhumation, rocks subducted to different depth can be mixed. Mixing of rocks with different metamorphic grade during the rocks exhumation was earlier recognized in the Dbie-Sulu orogenic belt (Zheng et al., 2005) Western Alps (Bousquet, 2008) as well as in the numerical simulations (Stöckhert and Gerya, 2005; Yamato et al., 2008).

As stated above the zircons with the detrital cores from sample Mu-93-10 suggest that this two-mica schist can be regarded as a fragment of the reworked crust of the Siberian craton. We believe that fragments of the crust of the Siberian craton could be involved in the subduction zone during either the continental subduction (Stöckhert and Gerya, 2005; Stern, 2011; Keppie et al., 2012) or its exhumation.

6. Conclusions

Integration of zircon U-Pb dating with its Hf-isotope composition and whole-rock Nd isotopes suggests a heterogeneous structure for the eclogite-gneiss complex of the North Muya dome. In addition to the rocks that experienced the eclogite-facies metamorphism (650–630 Ma) the metamorphic rocks of the eclogite-gneiss complex also include metapelites that experienced the last tectonothermal event at 800 Ma.

Based on isotopic data we conclude that Neoproterozoic gneisses and schist of the North Muya dome characterized by reworking of Paleoproterozoic and Archean crust with additions of juvenile material. The earliest Paleoproterozoic (2.1 and 1.9 Ga) and Neoproterozoic (800–850 Ma) stages, which involved the remelting of Archean crust and addition of juvenile material, are shown only in zircons from two-mica schist (Mu-93-10). The detrital zircons from this sample, with U-Pb ages ranging from 1.9 to 3.3 Ga and Hf model ages scattered from 0.81 to 3.86 Ga, may suggest that the protoliths of those rocks were part of the passive margin of the Siberian craton.

At the same time, zircons from granitic gneisses of the North Muya dome show a relatively narrow spread in crystallization age, with the major peak at 760 Ma. Hf-isotope model ages of zircons and Nd model ages for gneisses indicate a significant input of a

Neoproterozoic juvenile component in the protoliths of the granitic gneisses.

The eclogite-gneiss complex of the North Muya block marks the transition from the oceanic subduction to the collision of island arcs with the continental blocks that separated from Rodinia or with the margin of the Siberian craton.

Acknowledgements

We are grateful to W.L. Griffin for productive discussions that significantly improved the quality of the manuscript. Vladislav Shatsky and Sergei Skuzovatov were partially supported by the Siberian Branch of the Russian Academy of Sciences (integration project No. 49) and Russian Foundation for Basic Research (Grant No. 13-05-00261). Vladimir Malkovets was partially supported by Russian Foundation for Basic Research (grants No. 12-05-33035, 13-05-01051 and 15-05-05615). Elena Belousova acknowledges ARC support through FT110100685. This study was funded by Australian Research Council (ARC) grants and funding to the ARC Centre of Excellence for Core to Crust Fluid Systems (CCFS), and used instrumentation funded by the Australian Research Council, ARC LIEF grants, NCRIS, DEST SII grants, Macquarie University and industry sources. This is contribution 583 from the ARC Centre of Excellence for Core to Crust Fluid Systems (<http://www.ccfs.mq.edu.au>) and 989 in the GEMOC Key Centre (<http://www.gemoc.mq.edu.au>). We thank two anonymous referees for constructive and thoughtful comments. Our great thanks to Anastasia Gibsher for technical help with portions of the manuscript. We thank Prof. W.L. Griffin for editing the English.

References

- Avchenko, O.V., Kozyrev, I.V., Travlin, L.V., 1988. Metamorphism of gneiss complex of the North Muya block: Middle-Vitim mountain land. *Geol. Geophys.* 6, 82–89 (in Russian).
- Belousova, E.A., Reid, A.J., Griffin, W.L., O'Reilly, S.Y., 2009. Rejuvenation vs. recycling of Archean crust in the Gawler Craton, South Australia: evidence from U-Pb and Hf isotopes in detrital zircon. *Lithos* 113, 570–582.
- Bulgatov, A.N., 1988. Geologic-geophysical model of the upper part of the crust, Northern Transbaikalia. *Geol. Geophys.* 9, 62–68 (in Russian).
- Bulgatov, A.G., Gordienko, I.V., 1999. Terranes of the Baikal mountainous region and location of gold deposits. *Geol. Ore Depos.* 41 (3), 230–240 (in Russian).
- Burov, E., Francois, T., Yamato, P., Wolf, S., 2014. Mechanisms of continental subduction and exhumation of HP and UHP rocks. *Gondwana Res.* 25, 464–493.
- Bousquet, R., 2008. Metamorphic heterogeneities within a single HP unit: overprint effect or metamorphic mix? *Lithos* 103, 46–69.
- Cawood, P.A., Kröner, A., Collins, W.J., Kusky, T.M., Mooney, W.D., Windley, B.F., 2009. Accretionary orogens through Earth history. *Geological Society, London, Special Publications* 318, 1–36.
- Dobretsov, N.L., Gabov, N.F., Dobretsova, L.V., Kozyreva, N.V., 1989. Eclogite-like rocks (drusites) and eclogites in Precambrian blocks in Baikal region. In:

- Dobretsov, N.L., et al. (Eds.), Eclogites and Glaucophane Schist in Fold Regions. Nauka, Novosibirsk, pp. 7–34 (in Russian).
- Ernst, W.G., 2001. Subduction, ultrahigh-pressure metamorphism, and regurgitation of buoyant crustal slices – implications for arcs and continental growth. *Phys. Earth Planet. Inter.* 127, 253–275.
- Griffin, W.L., Pearson, N.J., Belousova, E.A., Jackson, S.R., van Achterbergh, E., O'Reilly, S.Y., Shee, S.R., 2000. The Hf isotope composition of cratonic mantle: LAM-MC-ICPMS analysis of zircon megacrysts in kimberlites. *Geochim. Cosmochim. Acta* 64, 133–147.
- Griffin, W.L., Belousova, E.A., Shee, S.R., Pearson, N.J., O'Reilly, S.Y., 2004. Archean crustal evolution in the northern Yilgarn Craton: U-Pb and Hf-isotope evidence from detrital zircons. *Precambrian Res.* 131, 231–282.
- Keppie, J.D., Nance, R.D., Dostal, J., Lee, J.K.W., Ortega-Rivera, A., 2012. Constraints on the subduction erosion/extrusion cycle in the Paleozoic Acatlán Complex of southern Mexico: geochemistry and geochronology of the type Piaxtla Suite. *Gondwana Res.* 21, 1050–1065.
- Kovalenko, V.I., Yarmolyuk, V.V., Kovach, V.P., Kotov, A.B., Kozakov, I.K., Salnikova, E.B., Larin, A.M., 2004. Isotope provinces, mechanisms of generation and sources of the continental crust in the Central Asian mobile belt: geological and isotopic evidence. *J. Asian Earth Sci.* 23 (5), 605–627.
- Kröner, A., Kovach, V., Belousova, E., Hegner, E., Armstrong, R., Dolgopolova, A., Seltmann, R., Alexiev, D.V., Hoffmann, J.E., Wong, J., Sun, M., Cai, K., Wang, T., Tong, Y., Wilde, S.A., Degtyarev, K.E., Rytsk, E., 2014. Reassessment of continental growth during the accretionary history of the Central Asian Orogenic Belt. *Gondwana Res.* 25, 103–125.
- Kylander-Clark, A.R.C., Hacker, B.R., Johnson, C.M., Beard, B.L., Mahlen, N.J., Lapen, T.J., 2007. Coupled Lu-Hf and Sm-Nd geochronology constrains prograde and exhumation histories of high- and ultrahigh-pressure eclogites from western Norway. *Chem. Geol.* 242, 137–154.
- Li, Z.H., Xu, Z.Q., Gerya, T.V., 2011. Flat versus steep subduction: contrasting modes for the formation and exhumation of high- to ultrahigh-pressure rocks in continental collision zones. *Earth Planet. Sci. Lett.* 301, 65–77.
- Liou, J.G., Ernst, W.G., Song, S.G., Jahn, B.M., 2009. Tectonics and HP-UHP metamorphism of northern Tibet – preface. *J. Asian Earth Sci.* 35, 191–198.
- Mezger, K., Essene, E.J., Halliday, A.N., 1992. Close temperature of the Sm–Nd system in metamorphic garnets. *Earth Planet. Sci. Lett.* 113, 397–409.
- Richard, A., Gurriet, P., Soudant, M., Albareda, F., 1985. Nd isotopes in French Phanerozoic shales: external vs. internal aspects of crustal evolution. *Geochim. Cosmochim. Acta* 49, 601–610.
- Rosen, O.M., Levskii, L.K., Zhuravlev, D.Z., Rotman, A.Y., Spetsius, Z.V., Makeev, A.F., Zinchuk, N.N., Manakov, A.V., Serenko, V.P., 2006. Paleoproterozoic accretion in the Northeast Siberian Craton: isotopic dating of the Anabar collision system. *Stratigr. Geol. Correl.* 14 (6), 581–601.
- Rubatto, D., Hermann, J., 2007. Zircon behavior in deeply subducted rocks. *Ele* 3, 31–35.
- Rytsk, E.Y., Amelin, Y.V., Rizvanova, N.G., Krimsky, R.S., Mitrofanov, G.L., Mitrofanova, N.N., Perelyaev, V.I., Shalav, V.S., 2001. Age of rocks in the Baikal-Muya Foldbelt. *Stratigr. Geol. Correl.* 9 (4), 3–15.
- Rytsk, E.Y., Kovach, V.P., Yarmolyuk, V.V., Kovalenko, V.I., 2007. Structure and evolution of the continental crust in the Baikal Fold Region. *Geotectonics* 41, 440–464.
- Rytsk, E.Y., Kovach, V.P., Yarmolyuk, V.V., Kovalenko, V.I., Bogomolov, E.S., Kotov, A.B., 2011. Isotopic structure and evolution of the continental crust in the East Transbaikalian segment of the Central Asian Foldbelt. *Geotectonics* 45, 349–377.
- Shatsky, V.S., Jagoutz, E., Ryboshlykov, Y.V., Koz'menko, O.A., Vavilov, M.A., 1996. Eclogites of the North Muya block: evidence of the Vendian collision in the Baikal-Muya ophiolite belt. *Doklady Earth Sci.* 350 (5), 677–680.
- Shatsky, V.S., Sitnikova, E.S., Tomilenko, A.A., Ragozin, A.L., Koz'menko, O.A., Jagoutz, E., 2012. Eclogite-gneiss complex of the Muya block (East Siberia): age, mineralogy, geochemistry, and petrology. *Russ. Geol. Geophys.* 53, 501–521.
- Shatskii, V.S., Skuzovatov, S.Y., Ragozin, A.L., Drill, S.I., 2014. Evidence of Neoproterozoic continental subduction in the Baikal-Muya fold belt. *Doklady Earth Sci.* 495 (1), 1442–1445.
- Scherer, E.E., Whitehouse, M.I., Müunker, C., 2007. Zircon as a monitor of crustal growth. *Elements* 3, 19–24.
- Song, S., Zhang, L., Niu, Y., Su, L., Song, B., Liu, D., 2006. Evolution from oceanic subduction to continental collision: a case study from the Northern Tibetan Plateau based on geochemical and geochronological data. *J. Petrol.* 47, 435–455.
- Stern, C.R., 2011. Subduction erosion: rates, mechanisms, and its role in arc magmatism and the evolution of the continental crust and mantle. *Gondwana Res.* 20, 284–308.
- Stöckhert, B., Gerya, T.V., 2005. Pre-collisional high pressure metamorphism and nappe tectonics at active continental margins: a numerical simulation. *Terra Nova* 17, 102–110.
- Taylor, S.R., McLennan, S.M., 1995. The geochemical evolution of the continental crust. *Rev. Geophys.* 33 (2), 241–265.
- Tsygankov, A.A., 2005. Magmatic Evolution of the Baikal-Muya Volcanic–Plutonic Belt in the Late Precambrian. Publishing House of SB RAS, Novosibirsk, pp. 303 (in Russian).
- Yamato, P., Burov, E., Agard, P., Le Pourhiet, L., Jolivet, L., 2008. HP-UHP exhumation during slow continental subduction: self-consistent thermodynamically and thermomechanically coupled model with application to the Western Alps. *Earth Planet. Sci. Lett.* 271, 63–74.
- Warren, C.J., Beaumont, C., Jamison, R.A., 2008. Modeling tectonic styles and ultra-high pressure (UHP) rock exhumation during the transition from oceanic subduction to continental collision. *Earth Planet. Sci. Lett.* 267, 129–145.
- Windley, B.F., Alexeiev, D.V., Xiao, W., Kröner, A., Badarch, G., 2007. Tectonic models for accretion of the Central Asian Orogenic Belt. *J. Geol. Soc. Lond.* 164, 31–47.
- Zheng, Y.-F., Zhou, J.-B., Wu, Y.-B., Xie, Z., 2005. Low-grade metamorphic rocks in the Dabie-Sulu orogenic belt: a passive margin accretionary wedge deformed during continent subduction. *Int. Geol. Rev.* 47, 851–887.
- Zorin, Y.A., Sklyarov, E.V., Belichenko, V.G., Mazukabzov, A.M., 2009. Island arc-back-arc basin evolution: implications for Late Riphean-Early Paleozoic geodynamic history of the Sayan-Baikal folded area. *Russ. Geol. Geophys.* 50 (3), 149–161.